ON THE IMPORTANCE OF VALVE MODELLING, REFLECTED PRESSURES, AND WALL FRICTION, IN CATHENA WATER HAMMER SIMULATIONS

T.G. Beuthe

Atomic Energy of Canada Limited
Whiteshell Laboratories
Pinawa, Manitoba, Canada R0E 1L0

ABSTRACT

The results of code and modelling developments outlined in this paper show that CATHENA can be used to accurately model the behaviour of valve slam generated water hammer if sufficient care and detail are used to model the characteristics of the valve. It also shows that CATHENA can accurately predict the reflection and transmission of travelling water pressure waves at expansions, contractions, and dead ends. Finally, although CATHENA is capable of accurately predicting the critical phenomena observed in water hammer, the inter-peak timing of the pressure excursions is not well predicted when significant bulk flows occur. The use of an unsteady wall friction factor to correct for this discrepancy has been examined, but the implementation of relationships suggested in the literature provided too much damping. A good match between experimental and simulation data can be achieved, but it is suggested that the default implementation of such a relationship should take place only after an investigation of further potential loss terms can be completed.

1 INTRODUCTION

If CATHENA is to be used as a two-phase water hammer simulation tool, it must be able to accurately model the event initiating the water hammer, as well as modelling the reflections of the generated travelling pressure waves as they pass through area changes and reach dead ends. In the following sections, comparisons between experimental results and analytical solutions are made to CATHENA simulations to show the degree to which CATHENA can satisfy these requirements. In the first section, simulations are outlined which illustrate the accuracy with which CATHENA can model a water hammer pressure excursion caused by a slammed valve, and the required accuracy of the valve model used. In the second section, an analytical solution for water hammer pressure waves is compared with CATHENA simulations of travelling pressure waves passing through an expansion, a contraction and reflecting from a dead end.

The final section of this paper deals with the issue of the wall shear forces experienced as water hammer pressure waves travel through a system. The inadequacy of steady-state wall shear terms for simulating water hammer experiencing significant bulk fluid flows is discussed. A summary of the available literature on unsteady wall shear is provided, and CATHENA simulations are used to illustrate and discuss the effect of implementing an unsteady wall shear term into the code.

2 CATHENA

CATHENA (Canadian Algorithm for THErmalhydraulic Network Analysis) is a computer program developed by AECL at Whiteshell Laboratories (WL) primarily for the analysis of postulated LOCA events in CANDU reactors. CATHENA uses a transient, one-dimensional two-fluid representation of two-phase flow in piping networks. In the thermalhydraulic model, the liquid and vapour phases may have different pressures,

velocities, and temperatures. The thermalhydraulic model consists of solving six partial differential equations for the conservation of mass, momentum, and energy for each phase. Interface mass, energy, and momentum transfer between the liquid and vapour phases are specified using constitutive relations obtained either from the literature or developed from separate-effects experiments.

The code uses a staggered-mesh, one-step, semi-implicit, finite-difference solution method, that is not transit time limited. The extensive wall heat transfer package can account for radial and circumferential conduction, solid-solid contact, thermal radiation, pressure tube deformation, and the zirconium-steam reaction. The heat transfer package is general and allows the connection of multiple wall surfaces to a single thermalhydraulic node. The CATHENA code also includes component models required for complete loop simulations such as pumps, valves, tanks, break discharges, separator models, and an extensive control system modelling capability. A more complete description of the CATHENA thermalhydraulic code is provided in [1].

3 VALVE MODELLING UNDER WATER HAMMER CONDITIONS

When simulating water hammer created by a slammed valve it is important to examine the level of detail needed to accurately capture the phenomena. In early CATHENA water hammer simulations, an "instantly open" valve was used to model experiments performed at the Seven Sisters water hammer facility in which water hammer was created by collapsing a void at the high-point in the piping [2]. At the time these simulations were performed, the detailed characteristics of the valve used in the experiments were unknown, and the "instantly open" assumption did not affect the overall conclusions drawn from the simulations. However a closer examination of the results revealed some of the shortcomings of this simple valve model. As shown in Figure 1 for example, neither the arrival time, nor the shape of the initial pressure excursion were accurately simulated.

To address these shortcomings, an effort was made to develop a more detailed valve model to be used for all subsequent simulations of experiments performed at the Seven Sisters facility. Initially, an attempt was made to use the manufacturer's published specifications for the valve to create a CATHENA valve model, but the results proved to be inadequate.

To improve on the manufacturer's specifications, a CATHENA valve model was assembled using a detailed computer aided design (CAD) model of the high-speed 2-inch full bore valve used in all Seven Sisters Experiments. To obtain dimensions for the CAD model, a detailed inspection of the valve was made that provided accurate measurements of all the working parts of the valve. Based on these measurements, a CAD model was designed and used to calculate the open area of the valve as a function of open angle. As shown in Figure 2, the model included the presence of the ball, the valve body, and the valve seal. The open area was calculated as a projection from the lip of the ball to the edge of the seal. This projection was rotated with the closing valve as indicated in Figure 3. The projected area was chosen to approximate the area perpendicular to the fluid flow as the valve closes. The backlash of the valve stem in the valve ball slot was also accounted for in the model.

While the CAD model was being designed, a series of fast closing (FC series) valve slam water hammer experiments were commissioned and performed in the 7-Sisters facility. In these tests, the fast closing valve was located at the high point in the experiment. A water flow was established for each experiment, and the quick-acting valve was slammed shut, generating an initial pressure excursion created only by the action of the closing valve. These tests could be used to validate the CATHENA valve model under water hammer conditions. In particular, experiments FC02, O6FC02 and FC08 from this test series were chosen as representative experiments against which all subsequent valve models were tested.

3.1 CAD Valve Model Results

Once the open area of the valve as a function of open fraction had been obtained it was used to construct an appropriate CATHENA valve model for the experiment in question. Initially, a model was designed using a single orifice CATHENA valve model. Use of this model improved the pressure pulse arrival timing with respect to the simple model described in Section 3 above, but did not produce an initial pressure rise curve whose shape satisfactorily matched the experiment.

A more detailed model was finally developed in which the action of the orifice ball was modelled using two orifice models separated by a pipe segment (to model the volume of water inside the ball itself) as shown schematically in Figure 4. As shown in Figure 5, the simulated pressure rise now arrives less than 3 ms faster than shown in the experimental results. Although this is well within the experimental error, some of the idealized assumptions made in the CAD valve model may also contribute to this discrepancy. For example, the model results indicate the valve is closed at approximately 76°. Further discussions with the valve manufacturer revealed that the valve should close at an angle closer to 80–85° however. Considering that the valve closes in 60–80 ms, the difference between the calculated and quoted closing angle may help to explain the arrival time difference between the modelled and experimental results.

3.2 Experimentally Derived Valve Model Results

Following the completion of the CATHENA CAD valve model, a series of calibration experiments were performed to accurately determine the valve characteristics of the high-speed 2-inch full bore valve used in Seven Sisters Experiments. The results obtained from these experiments were used to construct a CATHENA valve model. The performance of this valve model has been compared to the results of experiment FC02 in Figure 6. As shown here the timing is better than that exhibited by the CAD model in Figure 5. The experimental and modelled pressure profiles shown in Figure 6 are now within 2 ms of each other. The modelled pressure profile also follows the experimentally measured profile more closely than that shown in Figure 5.

3.3 Comparison of Experimentally Derived and CAD Valve Models

When comparing the CATHENA simulation results shown in Figures 5 and 6, it is interesting to note that the CAD model results exhibit a distinct double peak. Although hints of this double peak are contained in the experimentally measured data, it appears more as a "shoulder" than an actual peak. When the experimentally derived valve model is used, the first peak in the modelled pressure excursion is substantially reduced, and also takes on more of a "shoulder" attribute.

A study was performed to examine the differences between the CAD and experimentally derived CATHENA valve models which might account for this difference in simulation results. After some investigation, it was found that the difference in the final closing characteristic of the CAD designed model accounted for this difference in simulation results. Originally, it was estimated in the CAD model that the valve closes at approximately 76°. The experimental results show that the valve in fact closes at approximately 81°. This difference can be explained by considering that the CAD model did not account for any slight radii at the edge of the valve ball or the valve seat. Also, a perfect seal was assumed to occur the instant the ball closes over the edge of the valve seat. In addition, any dynamic shifting in the valve seal under the influence of the water flow has also been neglected in the CAD model. These assumptions may cause the CAD model to estimate a smaller closing angle.

If the CAD-derived characteristic curve is modified to account for the discrepancy in the closing angle the results obtained are significantly different than before. As shown in Figure 7, the initial peak shown in Figure 5 has been reduced, and the results are now comparable to those observed in the experimentally derived valve model shown in Figure 6.

4 REFLECTION/TRANSMISSION OF PRESSURE WAVES

When water hammer occurs, a pressure wave is generated which passes through the piping system being modelled. Any obstructions, changes in area, or dead ends in the piping system can cause reflections of the oncoming wave to take place. The mechanisms are analogous to those experienced in electrical flows when high frequency signals reach points in the circuit where there are impedance changes. A change in area in a piping system can be thought of as a change in fluid impedance for a pressure wave. As the wave passes through the area change, part of the wave is reflected back the way it came, and part is transmitted, travelling further along the initial path. The two resulting waves travel in opposite directions, and the pressure behind both is the same.

The manner in which the conservation relationships have been numerically modelled in CATHENA does not preclude the modelling of pressure waves as they pass through a change of area, or are reflected from a dead end. The objective here is to demonstrate that CATHENA is capable of accurately capturing this phenomenon by comparing it to the analytical expression describing reflected pressure waves.

4.1 Analytical Model

The expression for the transmitted and reflected pressure at a pipe area discontinuity from area A_o to A can be written as [3]:

$$\frac{\Delta P}{\Delta P_o} = \frac{2}{1 + \frac{A}{A_o}} \tag{1}$$

where ΔP_o is the change in pressure caused by the initial incoming pressure wave, and ΔP is the final change in pressure resulting after the transmitted and reflected waves have passed, as shown schematically for the case of an expansion and a contraction in Figures 8 and 9 respectively.

In the extreme case of a dead end, $A = 0$, and therefore equation 1 reduces to:

$$\Delta P = 2\Delta P_o \tag{2}$$

Thus, the change in pressure due to the reflected wave is twice the change in pressure of the incident wave at a dead end, as shown schematically in Figure 10.

If the incoming pressure wave is assumed to have been created as a result of an instantaneous single-phase water hammer event [4] and lossless transmission of the resulting pressure wave is assumed, the analytical model is complete. The water hammer pressure wave will propagate as a step function at the sonic velocity of the fluid, with reflected and transmitted pressures as given by equation 1. If CATHENA is capable of

modelling reflected and transmitted pressure waves correctly, simulated pressures should agree with the predictions of equations 1 and 2.

4.2 CATHENA Reflection/Transmission Simulations

To validate the operation of CATHENA, three test cases were assembled, one to model an expansion, one to model a contraction, and one to model the reflection from a pipe dead end. The schematic representations of these models are shown in Figures 11, 12, and 13 respectively. In all simulations, a nodalization of 1 m/node and a timestep of between 1.0×10^{-4} and 1.0×10^{-5} were chosen to ensure convergence.

4.2.1 Expansion

As shown in Figure 11, a model of two 20 m sections of pipe of two different diameters (PIPE1 is 0.254 m, PIPE2 is 0.127 m in diameter) was assembled to simulate the expansion. The pressure difference between the two boundary conditions was arranged in such a way that a small flow is created from left to right. The system pressure is close to 2.0 MPa initially, the water temperature was set at 25 °C, and the initial water velocity was 0.16 m/s in PIPE1, and 0.64 m/s in PIPE2.

A transient run was completed in which the valve located between PIPE2 and right boundary condition PBCR was initially closed. This simulates the effect of "instantaneously" closing the valve. As a result, a pressure wave is created with a pressure of 2.97 MPa, or a $\Delta P_o = 0.97$ MPa, as the water comes to a stop at the upstream face of the valve. This pressure agrees well with that predicted by the instantaneous water hammer equation [4].

The condition of the system prior to the arrival of the pressure wave at the area change is shown in Figure 14 at time $t = 0.008$ s. The pressure wave is propagating left to the area change. The presence of the area change is shown by a solid vertical line at position 20 m. When compared to the analytical solution, shown as a broken line, it is clear that the first order numerical solution CATHENA employs results in some diffusion of the instantaneous pressure change implied in the analytical solution. However, the speed of propagation of the wave and the magnitude of the generated pressure behind the wave is accurately captured by the simulation.

As the pressure wave reaches the expansion, both the reflected and transmitted waves leave a pressure of 2.39 MPa behind, or a $\Delta P = 0.39$ MPa as shown in Figure 15 at time $t = 0.02$ s. As a result, $\Delta P / \Delta P_o = 0.4$ and this matches the results of $\Delta P / \Delta P_o = 0.4$ predicted by equation 1. The speed of propagation of the pressure waves, and their magnitude are both still accurately captured after the reflection at the expansion has taken place when compared to the analytical solution shown in Figure 15.

4.2.2 Contraction

As shown in Figure 12, a model of two 20 m sections of pipe of two different diameters (PIPE1 is 0.127 m, PIPE2 is 0.254 m in diameter) was assembled to simulate the contraction. As with the expansion simulation above, the pressure difference between the two boundary conditions was arranged in such a way that a small flow is created from left to right. The system pressure is close to 2.0 MPa initially, the water temperature was set at 25 °C, and the initial water velocity was 0.64 m/s in PIPE1, and 0.16 m/s in PIPE2.

A transient run was completed in which the valve located between PIPE2 and right boundary condition PBCR was initially closed, again to simulate an "instantly" slammed valve. This creates a pressure wave with a

pressure of 2.24 MPa, or a $\Delta P_o = 0.24$ MPa, as the water comes to a stop at the upstream face of the valve. This pressure agrees well with that predicted by the instantaneous water hammer equation [4].

The condition of the system prior to the arrival of the pressure wave at the area change is shown in Figure 16 at time $t = 0.008$ s. The pressure wave is propagating left to the area change and the presence of the area change is shown by a solid vertical line at position 20 m. As in the expansion, a comparison with the analytical solution shows the diffusion in the pressure wave resulting from the the first order numerical method used in CATHENA. However, the speed of propagation of the wave and the magnitude of the generated pressure behind the wave is accurately captured by the simulation.

As the pressure wave reaches the contraction, both the reflected and transmitted waves leave a pressure of 2.386 MPa behind, or a $\Delta P = 0.386$ MPa as shown in Figure 17 at time $t = 0.02$ s. As a result, $\Delta P/\Delta P_o = 1.6$ and this matches the results of $\Delta P/\Delta P_o = 1.6$ predicted by equation 1. Again, the speed of propagation of the pressure waves, and their magnitude are both accurately captured after the reflection at the contraction when compared to the analytical solution shown in Figure 17.

4.2.3 Reflection at Dead End

As shown in Figure 13, a model of a single 20 m section of pipe 0.0254 m in diameter (PIPE) with a single boundary condition (PBCR) was assembled to simulate the reflection of a pressure wave off a pipe dead end. The fluid in the pipe is initially at 2 MPa and is quiescent.

A transient run was completed in which the pressure boundary condition PBCR was initially set at 3.5 MPa, or a $\Delta P_o = 1.5$ MPa to simulate the "instantaneous" opening of a valve to a higher pressure boundary condition. The resulting pressure wave propagates to the dead end at the left at position 0.0 m as shown in Figure 18 at time $t = 0.008$ s. Again, CATHENA does not accurately capture the pressure step change implied by the "instantaneous" valve opening shown in the analytical solution, but the speed of propagation and the pressure behind the approaching wave are accurately captured by the numerical simulation.

When the pressure wave reaches the dead end, it reflects, and the pressure created behind the reflected wave is now 5.0 MPa, or a $\Delta P = 3.0$ MPa as shown in Figure 19 at time $t = 0.02$ s. As a result, $\Delta P/\Delta P_o = 2.0$ and this matches the results of $\Delta P/\Delta P_o = 2.0$ predicted by equation 2. The post-reflected speed of propagation and pressure magnitude of the resulting wave are accurately captured when compared to the analytical solution shown in Figure 19

5 WALL FRICTION

In an earlier study [4], it was determined that the inter-peak timing of the pressure excursions caused by a water hammer event is relatively well predicted by CATHENA when single-phase water hammer is involved or when the amount of void generated in the system is small. In such cases, the pressure waves pass through the system under examination without causing significant bulk flow in the fluid. However, when increasing amounts of void are generated in the system, the bulk fluid flow also increases. Under these conditions, CATHENA tends to predict an inter-peak time larger than that indicated by experimental results. Subsequent examination of the potential factors affecting the inter-peak timing of the water hammer pressure excursions revealed the inter-peak timing was relatively insensitive to the bubble diameter (and therefore the condensation rate through the interface per unit volume), the vapour generation rate and the apparent density constitutive in the code. However, changes in flow resistance were shown to have a significant effect. Increasing wall friction or junction resistances decreases the inter-peak timing of the water hammer pressure excursions. This tends to

TABLE 1: SUGGESTED VALUES OF k

	k_a	k_d	Ref.
1	0.02	1.24	[8, 13]
2	0.449	0.449	[13]
3	0.36 (laminar)		
	-0.54 (turbulent)	-0.44 (turbulent)	[8]
4	-0.3	-0.58	[8]
5	-0.33	-0.52	[13]
6	-0.0072	-0.0038	[8]

lead to the conclusion that an additional loss term is at work under the highly unsteady flow conditions experienced during a water hammer event.

Simply altering the velocity dependent resistance factors does not provide the proper correction however as these friction factors were derived under steady state conditions. An examination of the literature shows that a number of authors have considered the problem of measuring and explaining the effect of unsteady flows on flow resistance [5]– [13]. These studies point to the inadequacy of steady state wall friction factors under unsteady flow conditions. Indications are that under accelerating and decelerating flow conditions such as those experienced in water hammer there is a significant change in flow resistance. The literature highlights the potential modification in velocity profiles in the region near the pipe wall under unsteady or transient flow which can have an effect on the skin friction [8, 9].

From the literature [13], an equation has been proposed for the unsteady friction factor f_u of the form:

$$f_u = f_s + k\frac{D}{V^2}\frac{dV}{dt} \tag{3}$$

or

$$\frac{f_u}{f_s} = 1 + k\frac{D}{f_s V^2}\frac{dV}{dt} = 1 + \frac{k}{2}\phi \tag{4}$$

where V is the liquid velocity, D is the pipe diameter, $\frac{dV}{dt}$ is the acceleration, k is an empirical constant, f_s is the quasi-steady friction factor and ϕ is an acceleration factor defined as

$$\phi = \frac{2D}{f_s V^2}\frac{dV}{dt} \tag{5}$$

Two values of k are quoted, one for accelerating flows k_a, and one for decelerating flows k_d. Unfortunately, widely different values of k have been proposed. As shown in Table 1, not only do the proposed values of k vary significantly in magnitude, they also vary in sign. Some researchers suggest that the unsteady friction f_u should increase when acceleration takes place and decrease when deceleration takes place (see entries 1 & 2 in Table 1), whereas others propose the opposite (see entries 3–6 in Table 1).

Equation 3 was implemented in a prototype version of CATHENA using the suggested values of k shown in Table 1, and tested using simulations of water hammer events in which significant amounts of void are generated. The results indicate that the implementation of the k values shown in entries 1–5 provide so much damping that the pressure excursions caused by the water hammer are all but eliminated. For example, Figure 20 shows a comparison between the experimental results of Seven Sisters experiment FC02 and a

CATHENA simulation with and without the implementation of equation 3 using the k values suggested by Shuy [13] (entry 5 in Table 1).

To investigate possible reasons for this large damping, detailed CATHENA simulation values of ϕ, and Reynolds number Re were examined and compared to Shuy's experimental results (the most extensive and wide ranging results presently available). From these simulations it is clear that the values of ϕ and Re calculated in the simulation far exceeded range experienced in the experiments used to derive the values of k. Whereas the Reynolds numbers shown in the simulation exceeded 300,000 Shuy's experiments only considered Re $\leq 150,000$. Similarly, the simulation values of ϕ were quite large, sometimes exceeding values of ± 100 or even ± 1000, whereas only a very small range of $-2 \leq \phi \leq 3$ was investigated in Shuy's experiments, due to experimental limitations.

Another question which arises is that of the non-symmetry of equations 3 and 4. Although the values of f_u can increase indefinitely if $\frac{k}{2}\phi$ in equation 4 becomes a large positive value, but can only decrease to zero, because negative values of f_u would be unphysical. In fact, given Shuy's suggested value of $k_a = -0.33$, ϕ cannot become more than $\phi \simeq 6$ before it no longer contributes any changes to the calculated value of f_u. Thus, equations 3 and 4 implicitly have lower bounds, and were implemented this way in CATHENA. No investigators have commented on the limits implied by these relations. If simulations are performed in which the value of ϕ is set to zero beyond a pre-determined threshold, the best match between experimental and simulation results is achieved by limiting $|\phi| \leq 70$ as shown in Figure 21. Unfortunately, the initial pressure excursion caused by the valve closure is underestimated.

If an upper limit is imposed on the value of ϕ, the best match between experimental and simulation results is achieved by limiting $|\phi| \leq 20$. As shown in Figure 22, the inter-peak times are well predicted (within 5 ms) and the initial pressure excursion caused by the slammed valve is underestimated less than the results shown in Figure 21.

If values of k are adjusted in an attempt to match the simulation results with experimental results, absolute values of less than 0.05 must be used. Even then, the results are less than satisfactory since either the inter-peak timing or the magnitude of the peaks can be matched but not both simultaneously as shown in Figure 23 for $k_a = k_d = -0.05$. This may seem to agree better with the suggested k values shown in entry 6 of Table 1. The authors of reference [8] are careful to emphasize these values were derived under pulse flow conditions, and as such were subject to a relatively high degree of uncertainty.

Given the above results, it is suggested that the inclusion of an unsteady wall friction relations like the one shown in equation 3 would be inappropriate at this time. Although unsteady wall friction has been posited analytically and proven to exist experimentally, the relatively limited range of Reynolds numbers and ϕ examined by these investigations precludes its use in CATHENA until additional potential loss terms due to such factors as fluid-structure interaction can be determined. Once this has been done, it may be possible to revisit the concept of introducing an unsteady wall friction as a closure term.

6 SUMMARY AND CONCLUSIONS

Results presented in this report show that CATHENA can be used to accurately model the behaviour of valves used under water hammer conditions if sufficient care and detail is used to model the characteristics of the valve. It is recommended that, wherever possible, an accurate, detailed, experimentally derived characteristic curve is used to create the model of the valve. As of a result of this work, a detailed CATHENA model of the valve used in the Seven Sisters experimental water hammer facility has been obtained for use in water hammer simulations.

If CATHENA is to successfully perform water hammer simulation of any kind, it must also be capable of accurately modelling the reflected and transmitted waves created when a travelling pressure waves passes through an area change or reaches a pipe dead end. In this paper, a series of small single-effects CATHENA test cases was created to model a pressure wave as it passes through an expansion, a contraction and as it hits a pipe dead end. These simulations are shown to be in excellent agreement with the results of the analytical model in all cases. CATHENA accurately captures the pressure propagation phenomena as a travelling pressure wave traverses an area change in a pipe, or reaches a pipe dead end.

Previous investigations tend to indicate that larger discrepancies in the inter-peak timing between simulated and experimental results can be expected with larger generated bulk flows in the water hammer. This discrepancy was found to be sensitive to factors affecting flow resistance. An examination of the available literature on the subject tended to agree with this assessment, and also suggests that additional wall friction due to the acceleration of the fluid under water hammer conditions, might provide the required additional factor. Unfortunately, the existing research provides conflicting advice on how acceleration and deceleration affects flow resistance, and a trial implementation of suggested relationships provided too much damping to be useful due to the relatively limited scope of the investigations. It is suggested that the default implementation of an unsteady wall friction term into CATHENA be postponed until investigations into further potential loss terms such as those caused by fluid-structure interaction have been completed.

ACKNOWLEDGEMENTS

Thanks go out to Randall Swartz and Dennis Byskal for their help and cooperation in the preparation of this report.

REFERENCES

1. B.N. Hanna, "CATHENA: A thermalhydraulic code for CANDU analysis", Nuclear Engineering & Design, 180 (1998) 113-131.
2. T.G. Beuthe. 1996. "Assessment of CATHENA for Simulating Two-Phase Water Hammer," Proceedings of the Fifth International Conference on Simulation Methods in Nuclear Engineering, September 8–11, 1996, Montreal, Canada, Volume 1, Session 2A.
3. F.J. Moody. 1986. "Non-Intuitive Fluid Dynamics from Reactor and Containment Technology", In Forum on Unsteady Flow - 1986, proceedings of the Winter Annual Meeting of the American Society of Mechanical Engineers, Anaheim, CA, USA, 1986 December 7–12, American Society of Mechanical Engineers, Fluids Engineering Division (Publication) FED vol. 39, pp. 19–21.
4. T.G. Beuthe, "CATHENA Study of Two-Phase Water Hammer Inter-Peak Timing", 20th CNS Nuclear Simulation Symposium, White Oaks Inn & Resort, Niagara-on-the-Lake, September 7–9, 1997.
5. M. Kawahashi, S. Sasaki, H. Anzai, M. Suzuki, "Unsteady, One-Dimensional Flow in Resonance Tube (With Wall Friction, Heat Transfer and Interaction on a Contact Surface)", Bulletin of the Japan Society of Mechanical Engineers, v. 17, n. 114(1974)1555–1563.
6. J.L. Achard, G.M. Lespinard, "Structure of the Transient Wall-Friction Law in One-Dimensional Models of Laminar Pipe Flows", Journal of Fluid Mechanics, v. 113 (1981) 283–298.
7. H.J. Lautheusser, M.F. Letelier, "Unified Approach to the Solution of Problems of Unsteady Laminar Flow in Long Pipes", Trans. ASME J. Appl. Mech., v. 50, n. 1(1983)8–12.
8. J. Kurokawa, M. Morikawa, "Accelerated and Decelerated Flows in a Circular Pipe", Bulletin of the JSME, v. 29, n. 249 (1986) 758–765.
9. A.E. Vardy, K.L. Hwang, "Characteristics model of transient friction in pipes", Journal of Hydraulic Research, v. 29, n. 5 (1991) 669–684.

10. K. Suzuki, T. Taketomi, S. Sato, "Improving Zielke's method of simulating frequency-dependent friction in laminar liquid pipe flow", Journal of Fluids Engineering, Transactions of the ASME, v. 113, n. 4, (1991) 569–573.
11. A.E.. Vardy, H. Kuo-Lun, J.M.B. Brown, "Weighting function model of transient turbulent pipe friction", Journal of Hydraulic Research, v. 31, n. 4 (1993) 533–544.
12. A.S. Elansary, W. Silva, H.M. Chaudhry, "Numerical and experimental investigation of transient pipe flow", Journal of Hydraulic Research, v. 32, n. 5 (1994) 689–705.
13. E.B. Shuy, "Wall shear stress in accelerating and decelerating turbulent pipe flows", Journal of Hydraulic Research, v. 34 n. 2 (1996) 173–183.

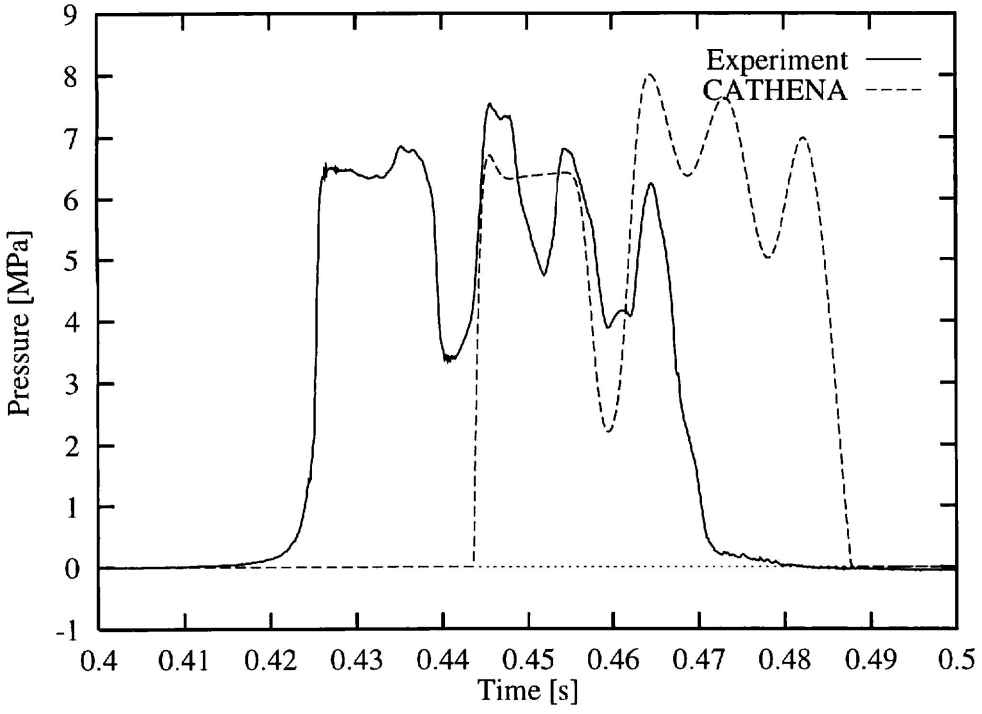

FIGURE 1: Comparison of Experimental Results (Seven Sisters Test T413E), and Simulation Results Obtained Using a Simple CATHENA Valve Model

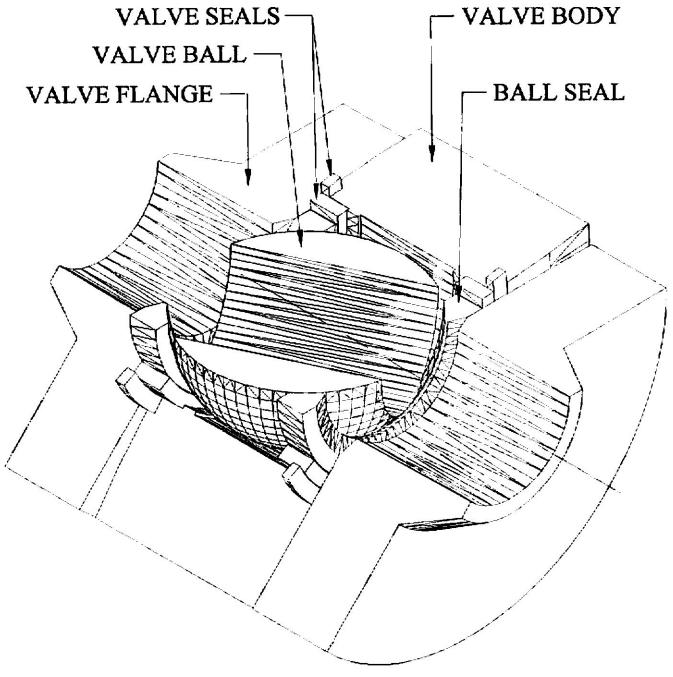

FIGURE 2: Detailed 3-D Cutaway of the Seven Sisters Valve CAD Model

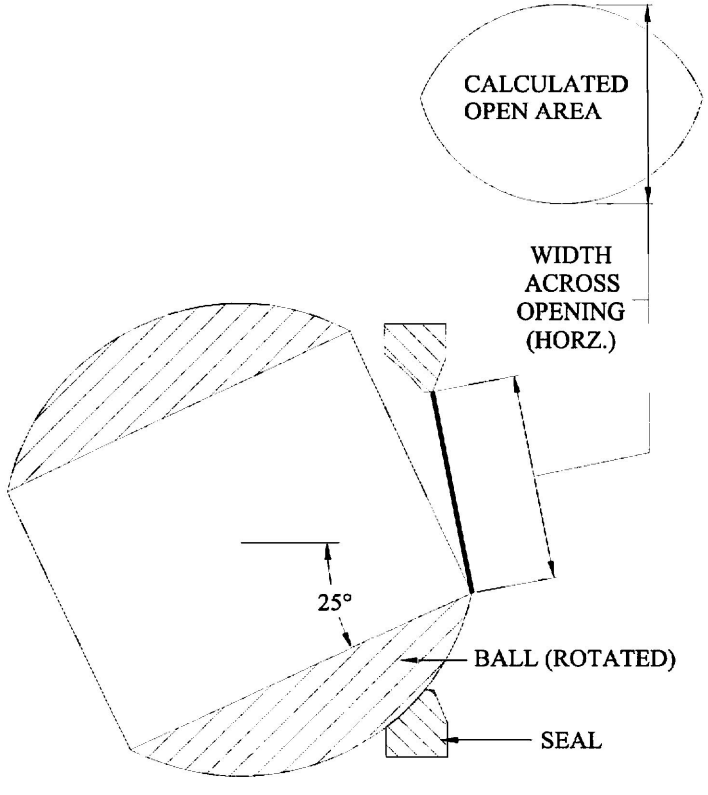

FIGURE 3: Seven Sisters Valve CAD Model Open Area Calculation

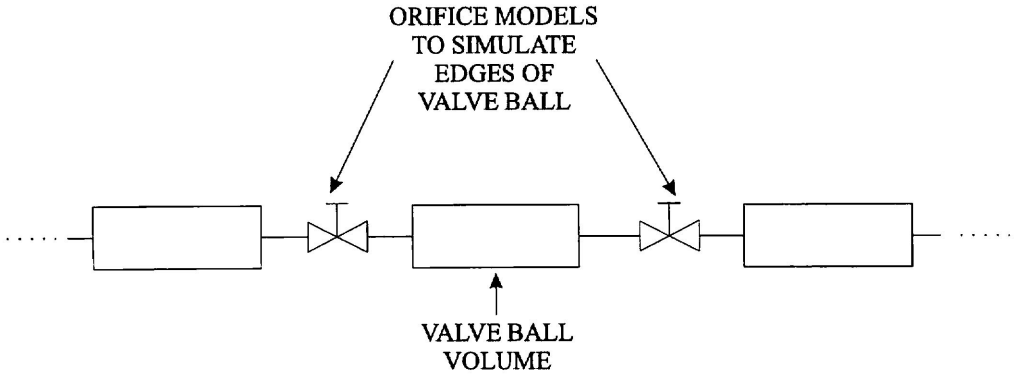

FIGURE 4: CATHENA CAD Valve Model Schematic

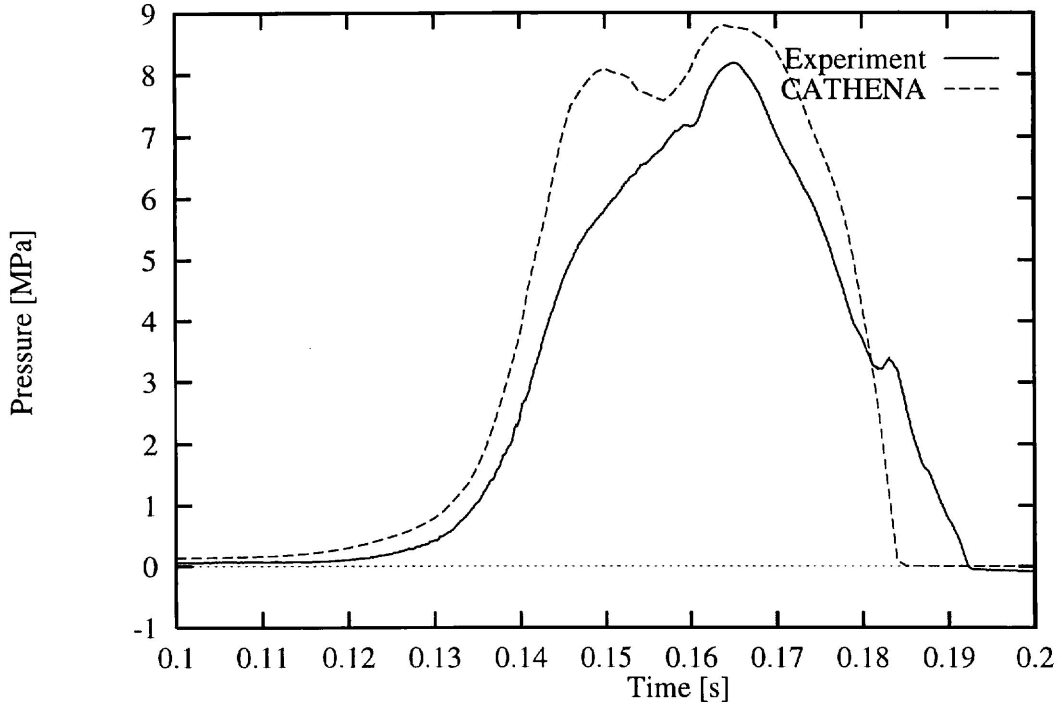

FIGURE 5: Comparison of Experimental Results (Seven Sisters Test FC02), and Simulation Results Obtained Using the CATHENA CAD Valve Model

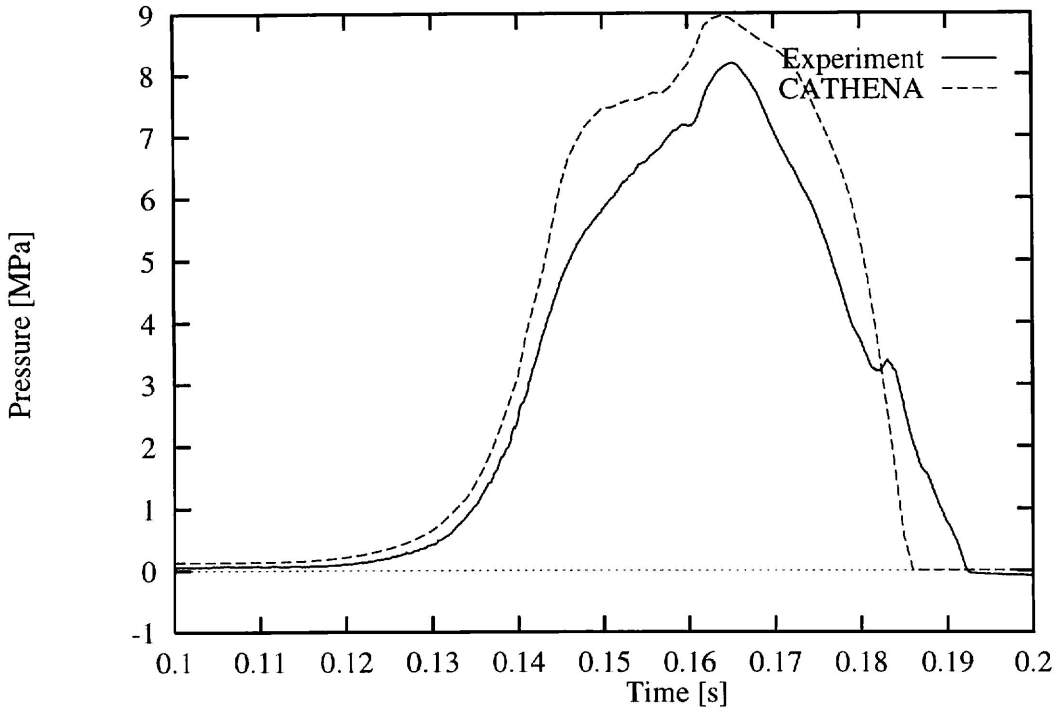

FIGURE 6: Comparison of Experimental Results (Seven Sisters Test FC02), and Simulation Results Obtained Using the Experimentally Derived CATHENA Valve Model.

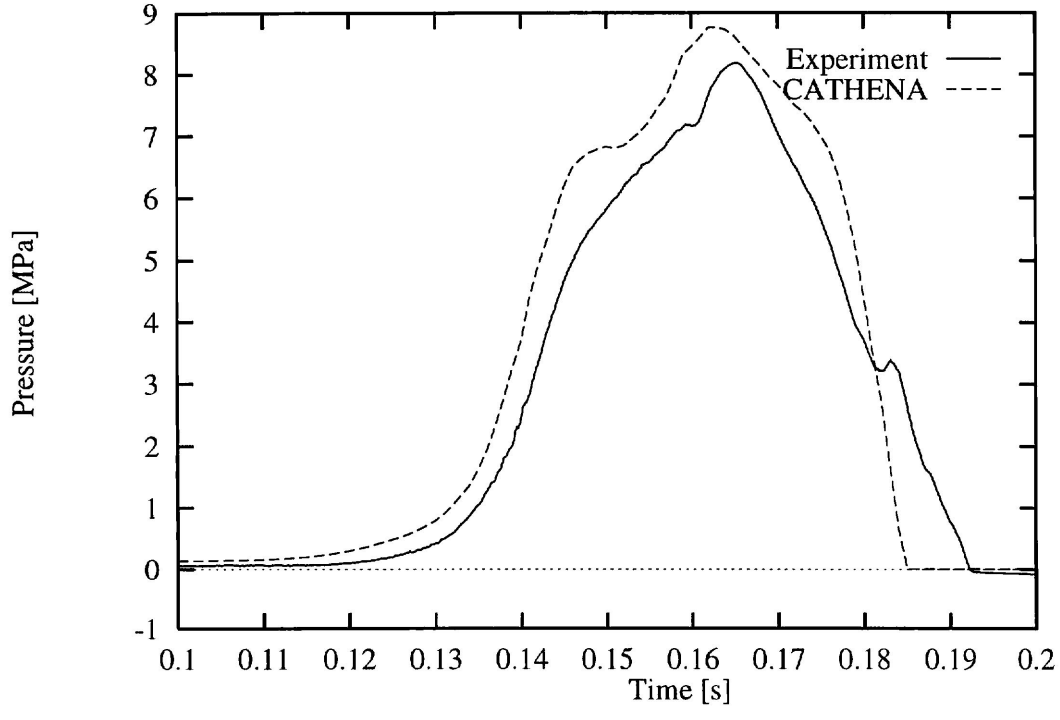

FIGURE 7: Comparison of Experimental Results (Seven Sisters Test FC02), and Simulation Results Obtained Using the CATHENA Modified CAD Valve Model which Accounts for the Experimentally Observed Closing Angle.

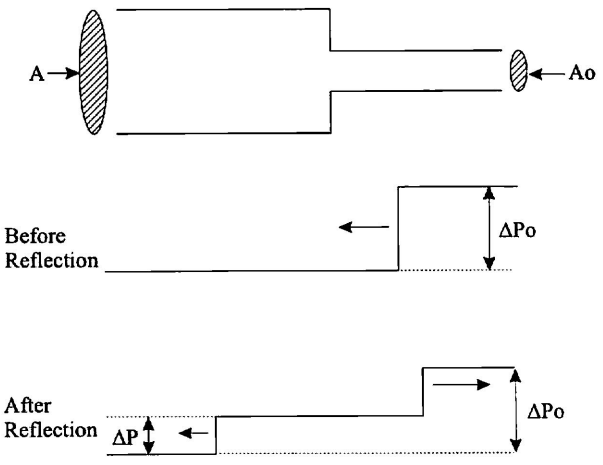

FIGURE 8: Pressure Wave Reflected from an Expansion.

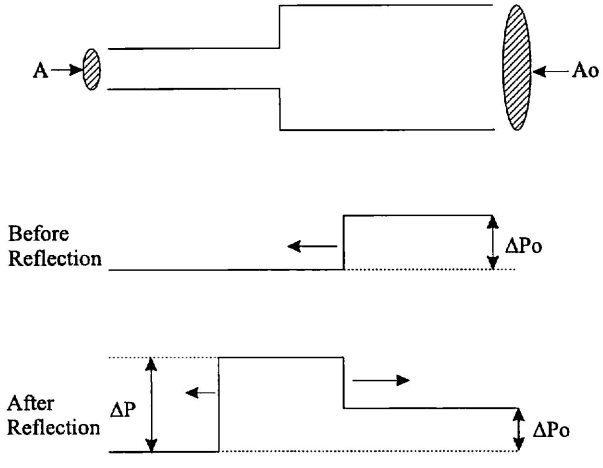

FIGURE 9: Pressure Wave Reflected from a Contraction.

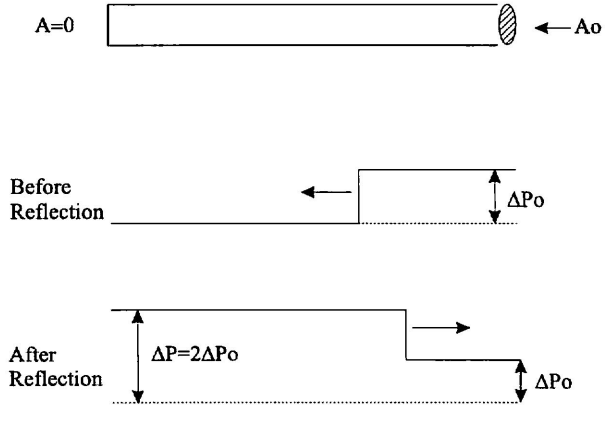

FIGURE 10: Pressure Wave Reflected from a Dead End.

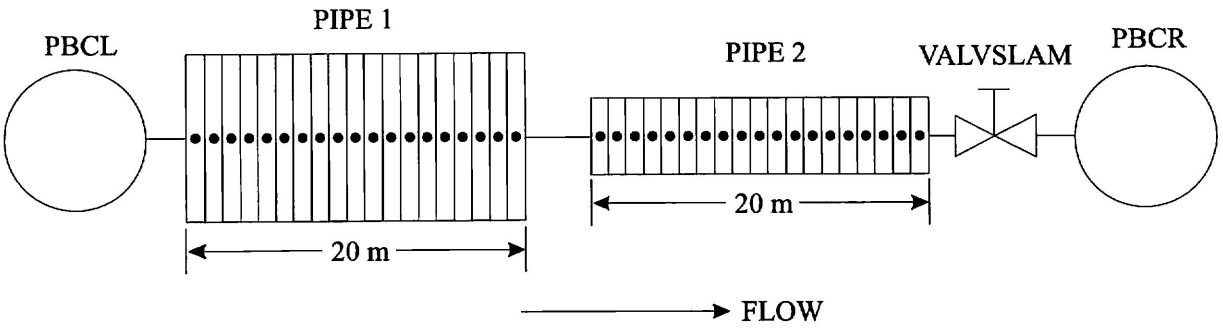

FIGURE 11: Schematic of the Expansion Model.

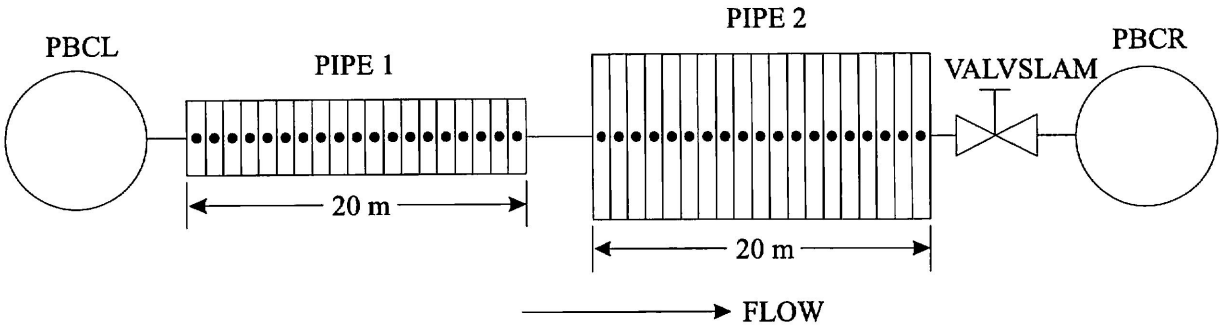

FIGURE 12: Schematic of the Contraction Model.

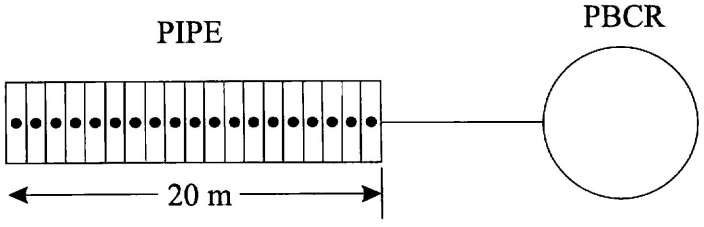

FIGURE 13: Schematic of the Dead End Model.

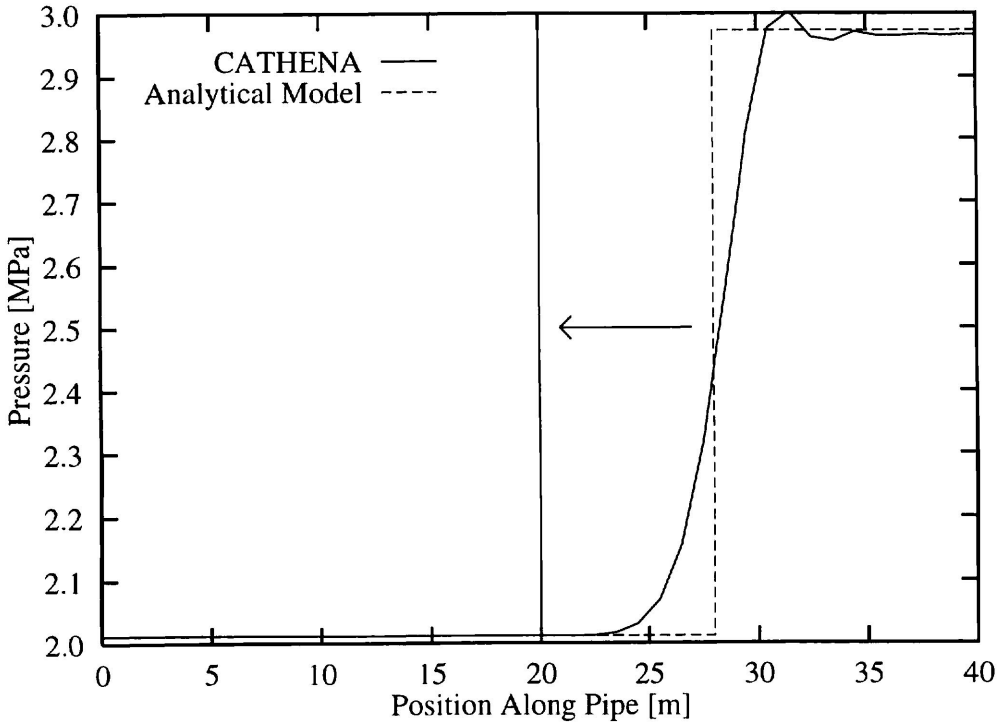

FIGURE 14: Approach of the pressure wave toward the expansion at $t = 0.008$ s.

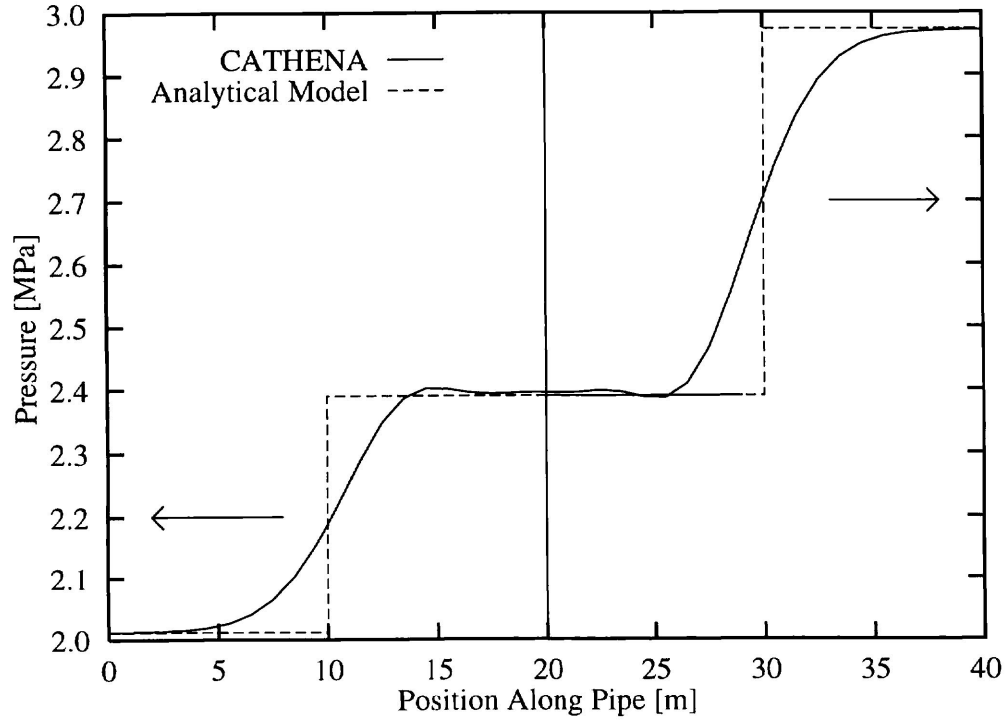

FIGURE 15: Pressure waves reflected and transmitted from the expansion at $t = 0.02$ s.

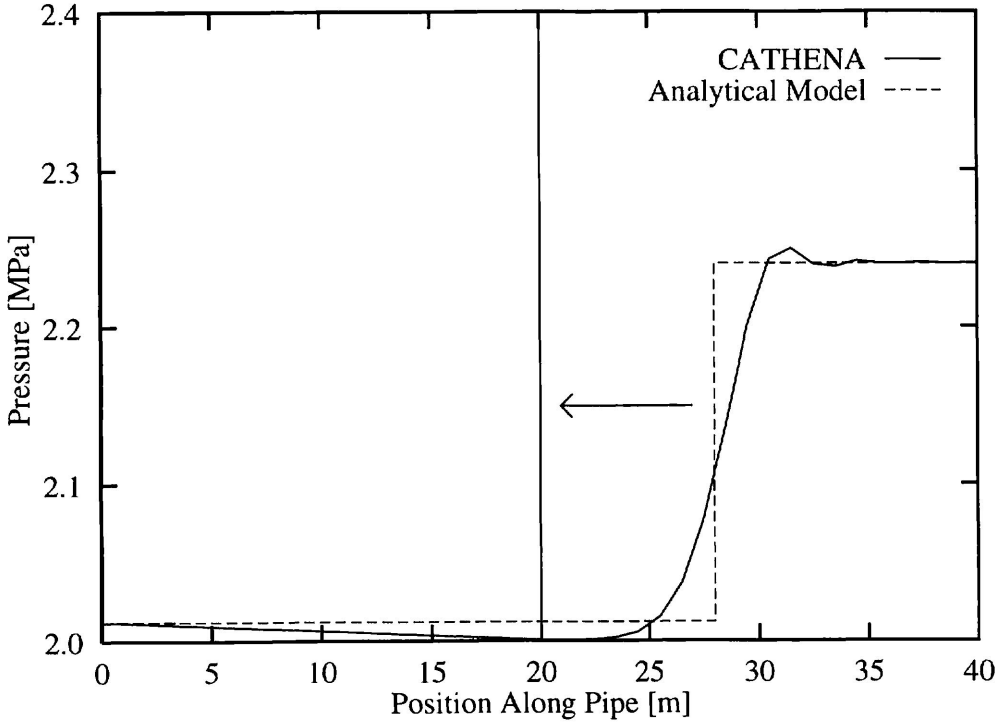

FIGURE 16: Approach of the pressure wave toward the contraction at $t = 0.008$ s.

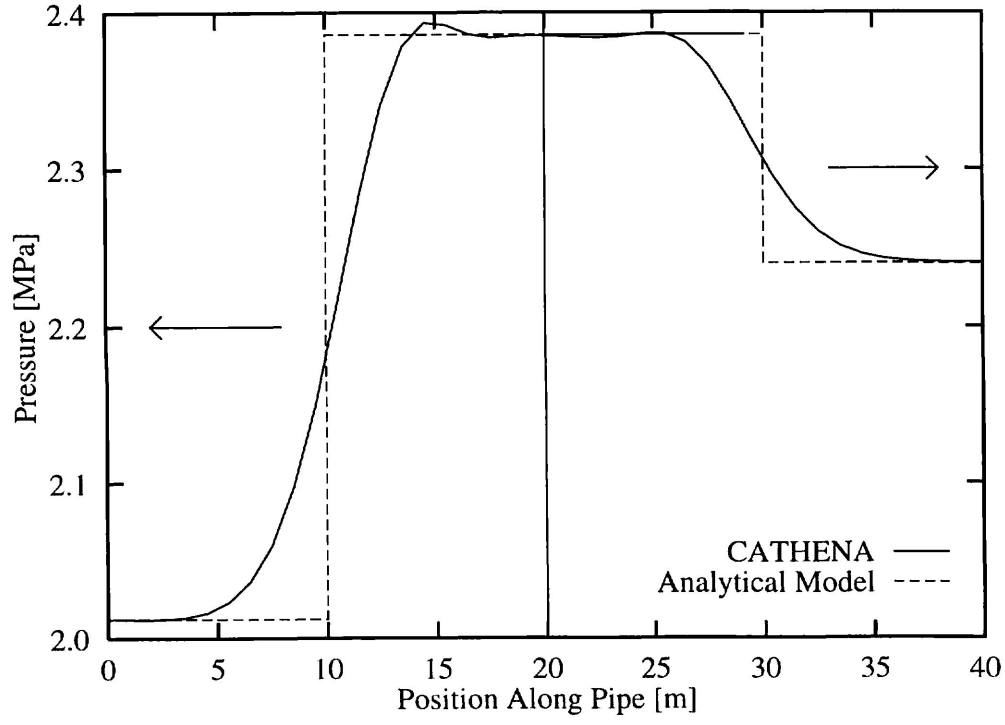

FIGURE 17: Pressure waves reflected and transmitted from the contraction at $t = 0.02$ s.

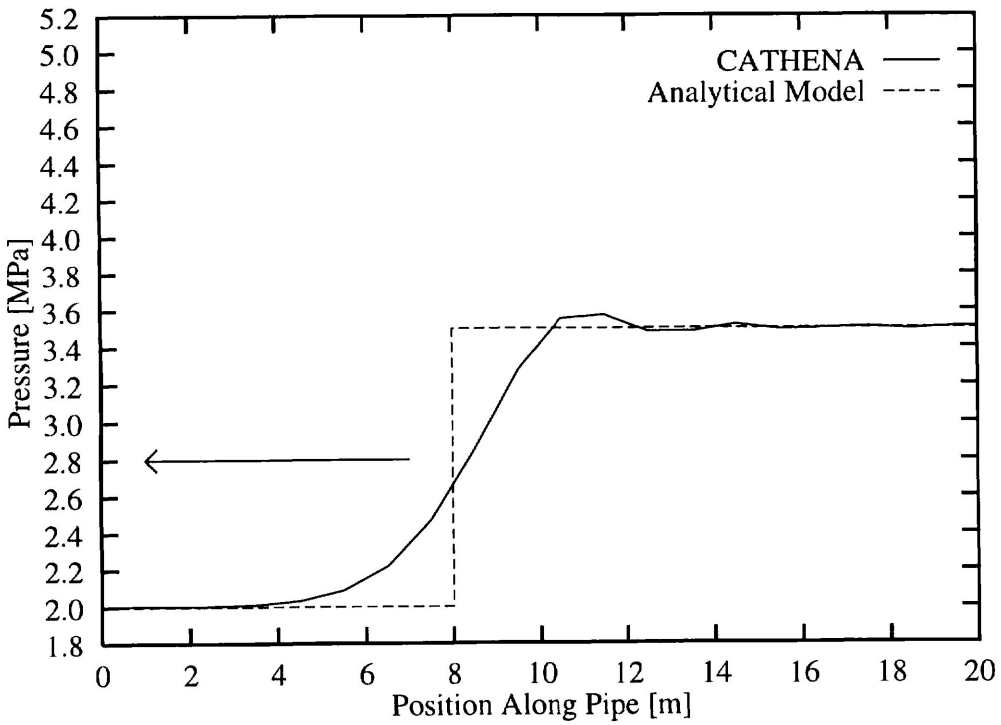

FIGURE 18: Approach of the pressure wave toward the dead end at $t = 0.008$ s.

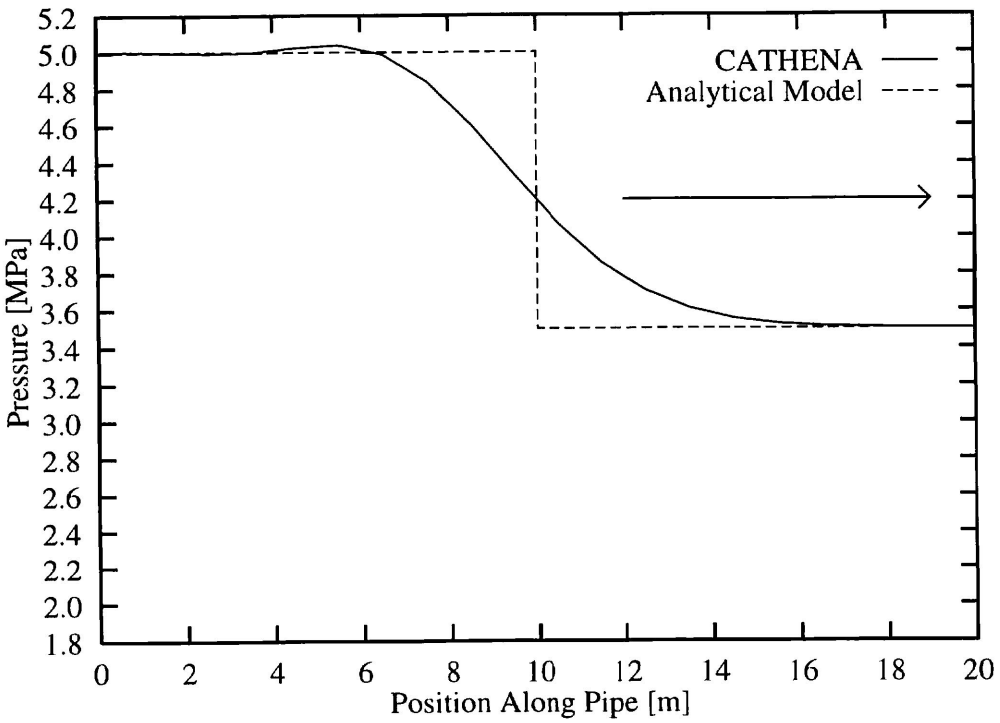

FIGURE 19: Pressure wave reflected from the dead end at $t = 0.02$ s.

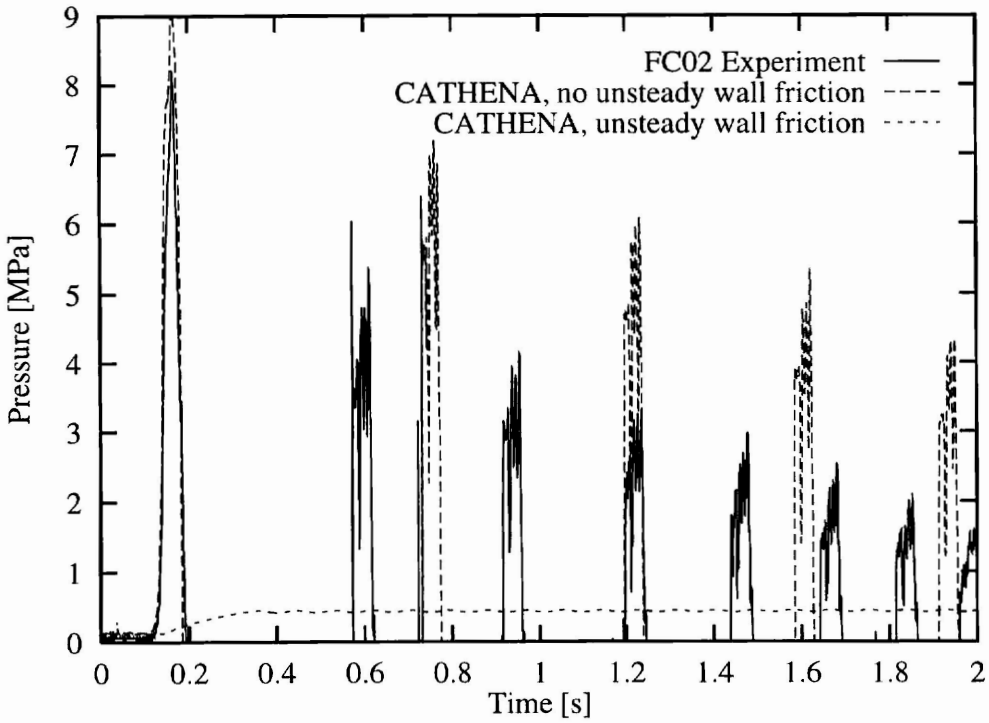

FIGURE 20: CATHENA simulation of Seven Sisters Experiment FC02 with and without unsteady wall friction by Shuy [13].

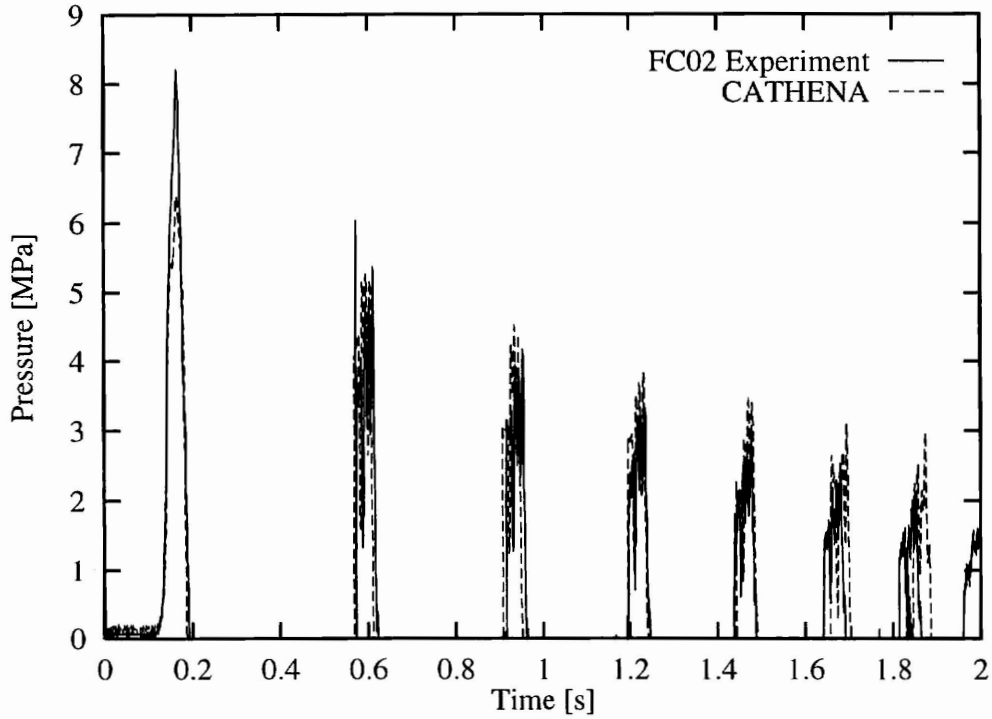

FIGURE 21: CATHENA simulation of Seven Sisters Experiment FC02 with unsteady wall friction by Shuy [13], and $|\phi| \leq 70$, zero otherwise.

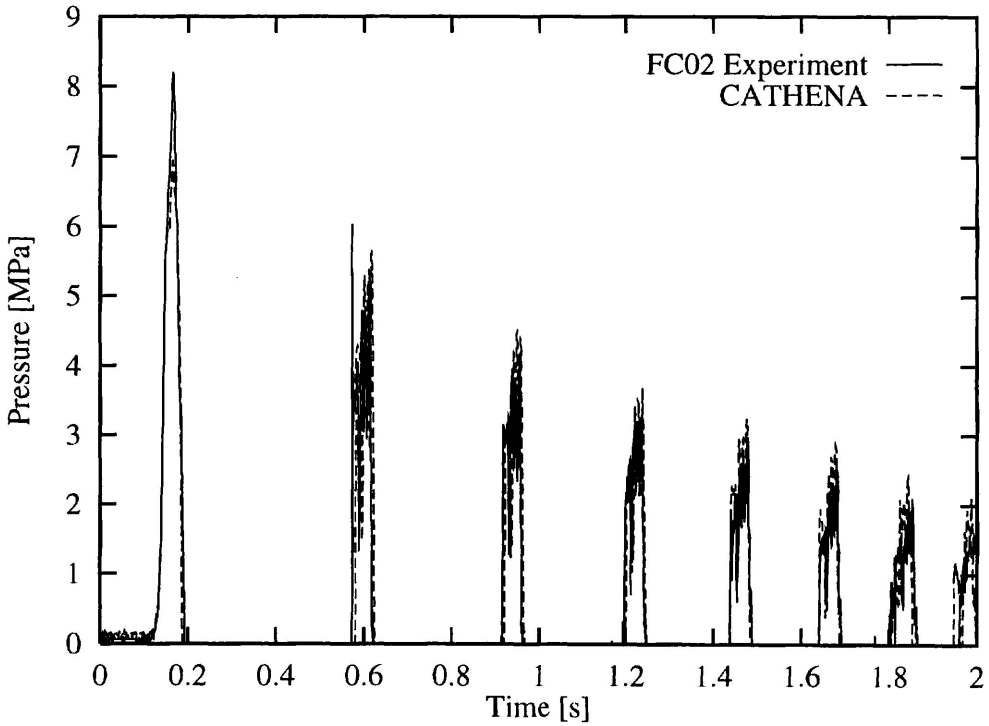

FIGURE 22: CATHENA simulation of Seven Sisters Experiment FC02 with unsteady wall friction by Shuy [13], and $|\phi| \leq 20$, $|\phi| = 20$ otherwise.

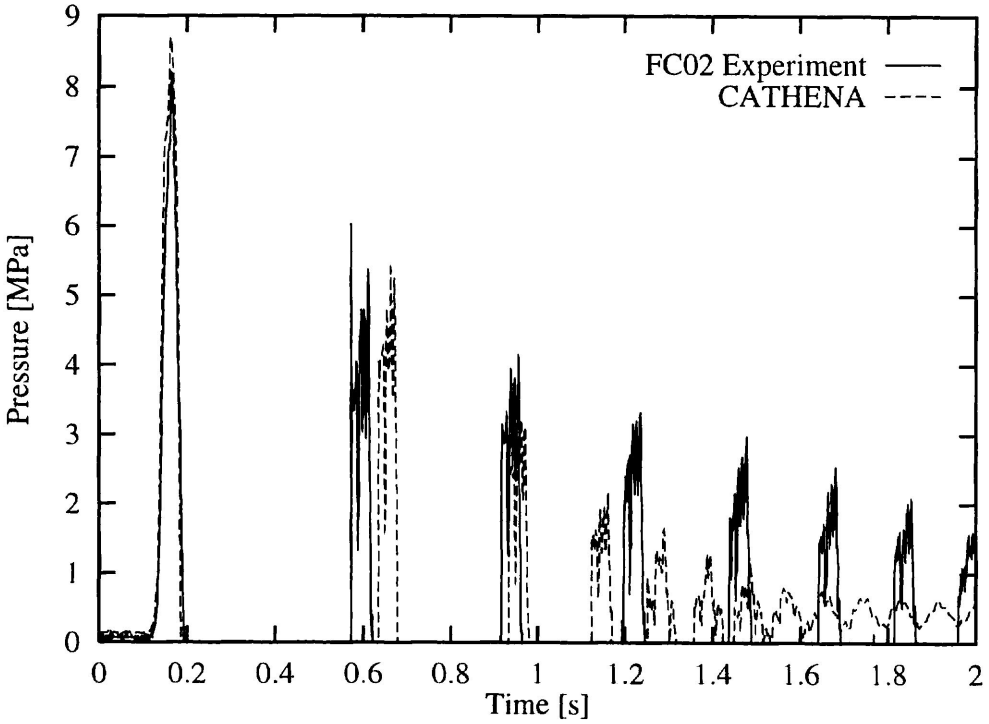

FIGURE 23: CATHENA simulation of Seven Sisters Experiment FC02 with unsteady wall friction by Shuy [13], and $k_a = k_d = -0.05$.